# Experimental analysis of an FAC-based coarsening scheme for open boundary problems

Daniel Ritter*, Ulrich Rüde*

January 16, 2011

**Abstract**

Poisson's equation on unbound domains was solved with a hierarchical grid coarsening approach based on Stephen F. McCormick's Fast Adaptive Composite grid method. We were especially interested in the efficient interface treatment with regular stencils this method enables. It was experimentally shown that the convergence properties are very similar to those of a fully refined grid scheme. The error behavior of a second-order scheme was empirically analyzed for an exemplary setup from molecular dynamics.

## 1 Introduction

Hierarchically coarsened grids play an important role in applications where problems need to be solved on a global domain. A variety of methods has been developed, starting either from a global coarse grid or from a local fine one to enable hierarchical structures with different grid sizes. One of these approaches is the Fast Adaptive Composite grid algorithm (FAC) that was introduced by Steve McCormick in [4]. It is not only a method that is very accurate in mathematical terms and can be easily implemented efficiently. In this efficient implementation it executes only regular stencil operations that operate only on one grid level at a time (except the grid transfer operations prolongation and restriction).
We developed a 2D code in the scripting language *python* to evaluate the numerical properties of the FAC in detail. The language was chosen due to its vectorization capabilities (similar syntax as MATLAB), its free availability and portability and the fact that the results can easily be visualized.
This article delivers an introduction to the model problem in section 2. The governing equation is covered as well as the applied concept of hierarchical grid coarsening. For this purpose, we introduce the necessary notation. In section 3 we describe and evaluate two setups that were run for analysis of convergence rates and the discretization errors of the FAC. Finally, an overview of next steps is given in section 4.

*Chair for System Simulation (Department of Computer Science 10), University of Erlangen-Nürnberg. Correspond to daniel.ritter@informatik.uni-erlangen.de.

# 2 Model description

Poisson's equation is a partial differential equation that appears in various problems in physics and engineering. In the following, a motivation from molecular dynamics (MD) is given. We will restrict to problems in 2D, i. e. $x = \binom{x^{(1)}}{x^{(2)}} \in \mathbb{R}^2$.

## 2.1 Poisson's equation on unbound domains

Assume a set of $N$ charged particles that are located within a bound area. The particles are approximated as point masses $m_i$ that are located at positions $x_i$ ($i \in \{1, 2, \dots N\}$). The charge $\rho_i$ of a particle can be modeled either by a point source (then $\rho_i$ is a Dirac impulse at position $x_i$) or by a smooth function with support on a bound area around $x_i$ (e. g. a Gaussian function or a polynomial). In the first case, numerical treatment is impractical due to the discontinuity at $x_i$ so that methods like the Zenger correction were developed ([8, 3]). These distribute the charge to direct neighboring grid points of $x_i$ if the space is discretized.
Let $\rho(x)$ be the superposition of all the particle charges $\rho_i$. From potential theory it is known that the acting forces at position $x$ can be derived from a global potential $\Phi(x)$ that is induced by $\rho(x)$. The governing equation for $\Phi(x)$ is also known as Poisson's equation and is given as

$$\Delta\Phi(x) = -\frac{1}{\varepsilon_0}\rho(x), \tag{1}$$

where $\varepsilon_0$ is the dielectricity. The operator $\Delta = \frac{\partial^2}{(\partial x^{(1)})^2} + \frac{\partial^2}{(\partial x^{(2)})^2}$ is called *Laplace operator*. From here, we will assume that the right-hand side $\rho(x)$ is modeled in an appropriate way (Zenger correction or smooth function) and that $\varepsilon_0$ is constant. We define $f(x) := -\frac{1}{\varepsilon_0}\rho(x)$ for reasons of simplicity.

In molecular dynamics the domain of $\Phi(x)$ is often considered to be unbounded, we also speak of *open boundary conditions*. Although the particles are moving within a bounded area, the induced field resides on an unbounded domain. If we are dealing with long-range interactions (e. g. Coulomb forces) this fact has to be considered in order to avoid unpredictable errors. The overall problem (including the b.c.s) can be formulated as

$$\Delta\Phi(x) = f(x),\ x \in \mathbb{R}^2, \text{ with } \Phi(x) \to 0 \text{ for } \|x\| \to \infty \tag{2}$$

where $\operatorname{supp}(f) \subset \Omega$ is a bounded subset of $\mathbb{R}^2$. $\Omega$ is also considered to be bounded and we will restrict to a square in the following. The boundary condition are a generalization of zero Dirichlet boundary conditions at infinity. A discrete formulation of this problem is given as

$$\Delta_h\Phi(x) = f(x),\ x \in \{x | x = h \cdot z, z \in \mathbb{Z}^2\}, \text{ with } \Phi(x) \to 0 \text{ for } \|x\| \to \infty, \tag{3}$$

where $h > 0$ is the grid size of the discretization and $\Delta_h$ is the discrete 5-point Laplace operator, i. e. at each grid point $x = \binom{x^{(1)}}{x^{(2)}}$ defined as

$$\Delta_h\Phi\begin{pmatrix}x^{(1)}\\x^{(2)}\end{pmatrix} := \frac{\Phi\binom{x^{(1)}+h}{x^{(2)}} + \Phi\binom{x^{(1)}-h}{x^{(2)}} + \Phi\binom{x^{(1)}}{x^{(2)}+h} + \Phi\binom{x^{(1)}}{x^{(2)}-h} - 4\,\Phi\binom{x^{(1)}}{x^{(2)}}}{h^2}. \tag{4}$$

Equation (3) constitutes a system of equations with an infinite number of unknowns.
A finite hierarchical coarsening approach can be applied in order to generate a problem of finite size [1, 7]. The starting point for this approach is the bounded domain $\Omega$. Different from [1], we perform the coarsening without decreasing the number of grid points, i. e. the physical diameter of the domain is doubled from level $i$ to $i+1$. This leads to an identical number of unknowns on the coarser levels. After applying several of those extending coarsening steps, we can use standard coarsening without domain extension in order to calculate the solution.

## 2.2 The Fast Adaptive Composite grid method for hierarchically coarsened grids

The great advantage of the FAC over the previous mentioned approaches is that all stencils are regular and therefore a straight-forward, efficient implementation on parallel architectures, such as GPGPUs is enabled. In [4] the FAC was introduced for adaptive refinement, but it can be applied just the other way round for hierarchical coarsening. Let us define a hierarchy of $K$ (continuous) domains as

$$\Omega_k := [-\tfrac{(n-1)}{2}h_k; \tfrac{(n-1)}{2}h_k] \times [-\tfrac{(n-1)}{2}h_k; \tfrac{(n-1)}{2}h_k], \quad \text{with } h_k = 2^k \cdot h,\ k \in \{0, 1, \dots K-1\}. \tag{5}$$

$\Omega_k$ is the square that has the origin at its center and the length $(n-1)h_k$, i. e. the subscript $k$ parametrizes its diameter. We now switch to discrete grids. Let

$$\Omega_k^h := \Omega_k \cap \{x | x = h \cdot z, z \in \mathbb{Z}^2\} \tag{6}$$

be the subset of the grid with mesh width $h$ that has the physical dimensions of $\Omega_k$. The superscript specifies the grid level, we are considering. To emphasis this even more we could say that $k$ describes the region of the grid and $h$ its mesh width.
Let ${}^{+}\Omega_k^h$ denote the grid $\Omega_k^h$ plus an additional outer layer of grid points (called *ghost layer* or *halo*). Accordingly, ${}^{++}\Omega_k^h$ is $\Omega_k^h$ plus two halo layers and ${}^{-}\Omega_k^h$ is the interior of $\Omega_k^h$. Note that the $^+$ and $^-$ always refer to the width $h_k$ which belongs to $k$, not to $h$. This may be an odd choice, but fits our requirements best.
A two-level example is given in figure 1. For solving equation 3 a hierarchical grid structure is created. Our FAC approach works with the following components:

- Pre-smoothing — using a red-black Gauss-Seidel (RBGS) smoother — is done on the interior ${}^{-}\Omega_k^{h_k}$ on the according level $k$.
- The residual is calculated on the domain and the first border, i. e. ${}^{+}\Omega_k^{h_k}$ and
- is transfered to the coarse grid frame ${}^{+}\Omega_k^{h_{k+1}}$. This means for the restriction that all values on ${}^{+}\Omega_k^{h_k}$ are taken into account (even of the halo), but the boundary of ${}^{+}\Omega_k^{h_{k+1}}$ is identical to that of $\Omega_k^{h_k}$ (since the halo points on the fine grid have no corresponding physical points on the coarse grid).

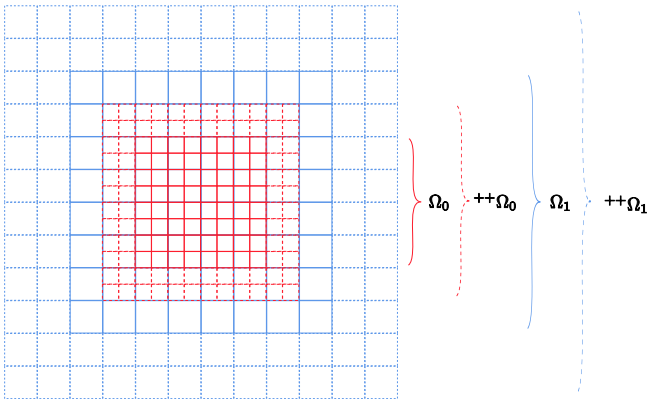


Figure 1: Two level coarsened grid

- After (recursively) solving the problem on the coarse grid, correction terms are prolongated from ${}^{++}\Omega_k^{h_{k+1}}$ to the fine domain and its first and second border ${}^{++}\Omega_k^{h_k}$.
- Finally, post-smoothing (RBGS) is done on the interior ${}^{-}\Omega_k^{h_k}$ again.

The implemented method is more complex: Since it may be necessary for our application to set non-zero boundary conditions on the coarsest grid, we do not restrict and solve the residual equation, but the original equation. This solution scheme is known as *Full Approximation Scheme* (FAS) [2]. Let $\tilde{I}_k^{k+1}$ be the full weighting restriction operator from level $k$ to level $k+1$, $\hat{I}_k^{k+1}$ the according direct injection operator and $I_{k+1}^k$ the bilinear interpolation operator (from level $k+1$ to $k$). $\Delta_h$ is the five-point Laplace operator with mesh size $h$ and $\Delta_h^{-1}$ its inverse, which can be established for given boundary conditions. $\nu_{\text{pre}}$ and $\nu_{\text{post}}$ are the numbers of pre- resp. post-smoothing steps. The values on the coarser levels $\Phi_k$, $r_k$ and $f_k$ for $k \in \{1, 2, \dots K-1\}$ are initialized with 0. As before let $h_k = 2^k \cdot h$. Then, a formal definition of the FAC method with $K$ levels is given in algorithm 1.

## 2.3 The FAC as restricted refinement scheme

The FAC can also be seen from another point of view that was developed implicitly by [4] and [6] and was formulated as adaptive relaxation in [5] (but for triangle meshes). Imagine a setup where the domain $\Omega_{K-1}$ is given with mesh size $2^{K-1}h$. The domain is now refined globally, i. e. in the previous notation the grids $\Omega_{K-1}^{2^{K-1}h}, \Omega_{K-1}^{2^{K-2}h}, \dots \Omega_{K-1}^{h}$ are used for solving the problem. This scheme leads to a classical multi grid scheme and is referred to as *fully refined scheme*. The relaxation (i. e. pre- and post-smoothing) is in a second step restricted like in the previous FAC scheme: On level $k$ it is now only performed on the sub-domain ${}^{-}\Omega_k^{h_k}$. This inner-point only relaxation is called *smoothed interior scheme*.
Now it is only one small step to the previously introduced *FAC*: All the remaining operations within the multi grid cycle — computation of the residual,

**Algorithm 1** FAC method

FAC$(k, K, \nu_{\text{pre}}, \nu_{\text{post}}, h)$:

**if** $(k = K - 1)$ **then**
  Calculate $\Phi_k$ exactly.
  **return**
**else**
  smooth $\Phi_k$ on ${}^{-}\Omega_k^{h_k}$ for $\nu_{\text{pre}}$ times
  compute residual on ${}^{+}\Omega_k^{h_k}$: $r_k \leftarrow f_k - \Delta_{h_k}\Phi_k$
  restrict residual $r_{k+1} \leftarrow \tilde{I}_k^{k+1} r_k$ for $r_{k+1} \in^{+} \Omega_k^{h_{k+1}}$
  restrict $\Phi_{k+1} \leftarrow \begin{cases} \hat{I}_k^{k+1}\Phi_k & \Phi_{k+1} \in^{++} \Omega_k^{h_{k+1}} \\ \Phi_{k+1} & \text{otherwise} \end{cases}$
  set $f_{k+1} \leftarrow \begin{cases} r_{k+1} + \Delta_{h_{k+1}}\Phi_{k+1} & \Phi_{k+1} \in^{++} \Omega_k^{h_{k+1}} \\ f_{k+1} & \text{otherwise} \end{cases}$
  call FAC$(k+1, K, \nu_{\text{pre}}, \nu_{\text{post}}, h)$
  compute error $e_{k+1} \leftarrow \Delta_{h_{k+1}}^{-1} f_{k+1} - \Phi_{k+1}$ on $\Omega_{k+1}^{h_{k+1}}$
  prolongate $e_k \leftarrow I_{k+1}^k e_{k+1}$ for $e_{k+1} \in^{++} \Omega_{k+1}^{h_{k+1}}$
  correct $\Phi_k \leftarrow \Phi_k + e_k$ on $\Omega_k^{h_k}$
  smooth $\Phi_k$ on ${}^{-}\Omega_k^{h_k}$ for $\nu_{\text{post}}$ times
**end if**

restriction, prolongation and correction — are also only done on the regarding subsets of the domain. Note that the smoothed interior and the FAC schemes are numerically equivalent. Evaluating the convergence rates for the three different schemes is part of the following section.

# 3 Numerical tests

There are two test cases in the focus within this section: First, we will estimate the smoothing properties of the FAC scheme using a noisy setup for the initial solution, before looking at the errors for a typical setup from MD, where the right-hand side is given by a Gaussian distribution. In this second case, the influence of the grid interfaces to the accuracy is also of interest.

## 3.1 Estimation of convergence rates

For getting an estimate for the convergence properties of the algorithm, we ran tests with the three different schemes using the following configuration: Two grid levels were used (one level of extension) and a V(3,3)-cycle was applied (i. e. three pre- and post-smoothing sweeps each). The following general setup was tested: The initial values of $\Phi_0(x)$ are set to uniformly distributed values between 0 and 1, while $f_0(x) = 0$. The boundary conditions are set to $\Phi_h(x_\delta) = 0$ for $x_\delta \in \delta\Omega_K^{h_K}$ [1]. The exact solution is $\Phi_0(x) = 0$. Since the approximate solution converges against zero, only a few V-cycles are possible before round-off errors would dominate the residual norms. To avoid this, the elements of

[1] Define the boundary as $\delta\Omega_K^{h_K} := \Omega_K^{h_K} \setminus^{-} \Omega_K^{h_K}$

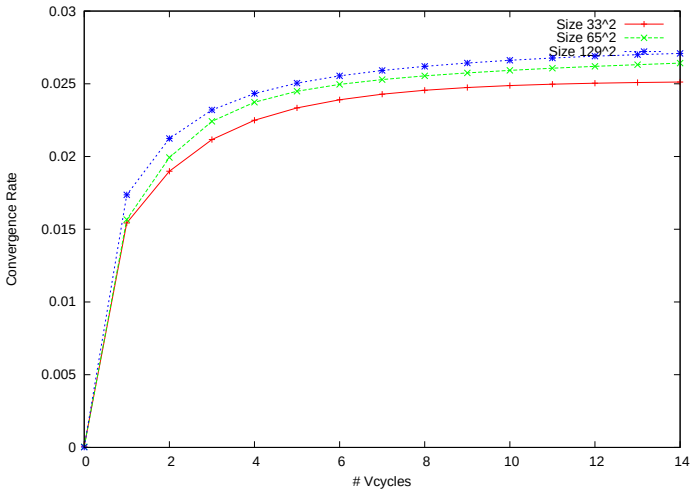


Figure 2: Convergence rates over iterations for Gaussian noise setup and two grid levels

Table 1: Convergence rates dependent on $\nu = \nu_{\text{pre}} = \nu_{\text{post}}$

| | Number of smoothing sweeps $\nu$ | | | | |
|---|---|---|---|---|---|
| | 1 | 2 | 3 | 4 | 5 |
| Convergence. rate | 0.071 | 0.040 | 0.027 | 0.021 | 0.017 |

the approximate solution vector are divided by its L2 norm after each V-cycle. We ran this test with the three different schemes introduced in subsection 2.3 for different sizes. The convergence rates are very similar in all cases and they are identical for the FAC and the smoothed interior scheme and differ only very slightly from the ones in the fully refined scheme. For $33^2$ unknowns, the convergence rate is 0.025 after a few iterations, for $65^2$ and $128^2$ it is 0.027. It is shown experimentally that the FAC achieves almost the same convergence as the fully refined scheme at a drastically reduced computational cost.

Figure 2 shows the convergence rates for the first 15 V-cycles for the FAC at different grid resolutions. It can be seen that the convergence rates are almost identical for all resolutions and that the convergence is far better during the first iterations.

We are interested in the convergence behavior for different numbers of pre- and post-smoothing sweeps. The idea is that an increased number of smoothing steps on each level yields a decreased residual, so the convergence should be better for more smoothing steps. In table 1 the convergence rates for different numbers of pre- and post-smoothing sweeps are displayed. These were generated with a grid resolution of $129^2$ . As expected, the convergence is better for more smoothing sweeps.

Table 2: Maximum (a) and L2 (b) error norms of the MD setup.

(a)

| Problem size | $33^2$ | $65^2$ | $129^2$ |
|---|---|---|---|
| Two-level scheme | 0.62 | 0.15 | 0.039 |
| Three-level scheme | 0.58 | 0.15 | 0.040 |
| Four-level scheme | 0.61 | 0.13 | 0.035 |

(b)

| Problem size | $33^2$ | $65^2$ | $129^2$ |
|---|---|---|---|
| Two-level scheme | 0.086 | 0.020 | 0.0051 |
| Three-level scheme | 0.093 | 0.020 | 0.0052 |
| Four-level scheme | 0.086 | 0.029 | 0.0059 |

## 3.2 Error analysis for a setup from molecular dynamics

Now a setup is tested that reflects a typical situation in molecular dynamics: A charged particle is placed at the origin and is modeled by a Gaussian function in the following way: The right-hand side is set to

$$f(x) = \frac{4}{r_{\text{cut}}^2}\left(\frac{||x||^2}{r_{\text{cut}}} - 1\right) e^{-\frac{||x||^2}{r_{\text{cut}}}},$$

where $r_{\text{cut}}$ scales the width of the distribution. We choose this case the smooth analytical solution is $\Phi(x) = \frac{1}{r_{\text{cut}}} e^{-\frac{||x||^2}{r_{\text{cut}}}}$ (if the boundary values are set accordingly). Effectively, the boundary values can set to zero for our tests since $\Phi(x)$ decays very fast. In case of long-range interactions, however, the potential behaves like $\frac{1}{||x||}$ for large $x$ and therefore an approximation formula may be required for real-world applications.
Tests were run with two, three and four grid levels and $r_{\text{cut}} = 0.02$. The domain of computation was $\Omega = [-\frac{1}{2}; \frac{1}{2}]^2$. V-cycles with three pre- and post-smoothing steps were executed for each number of grid levels. For test purposes, we solved the equation on the coarsest level with a sufficient number of RBGS cycles. The L2 and maximum norms of the absolute errors were calculated after each V-cycle and were found to remain constant after four iterations of the FAC. These final error norms are shown in table 2.

A look at the L2 norm of the residual, that is shown in figure 3 exemplary for the two level scheme and different resolutions, proves that the residual continues to converge for more iterations. Our explanation is that the accuracy of discretization error is reached after four V-cycles.
All cases show that the maximum norms of the error quarter roughly if the mesh width is doubled, i. e. an error order of $\mathcal{O}(h^2)$ is induced as expected. Also the L2 norm of the error is quartered if the resolution is doubled.

We now analyze the influence of the number of grid levels on the accuracy. Therefore, we compare the error for the different schemes at the same resolution.

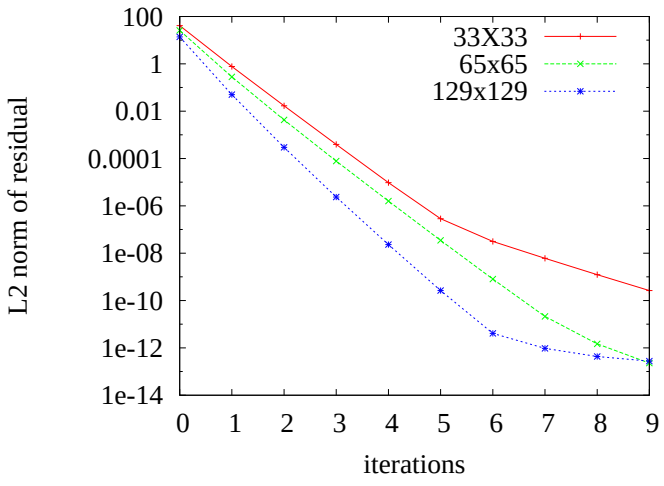


Figure 3: L2 norm of the residual for MD test setup and two level scheme at different resolutions.

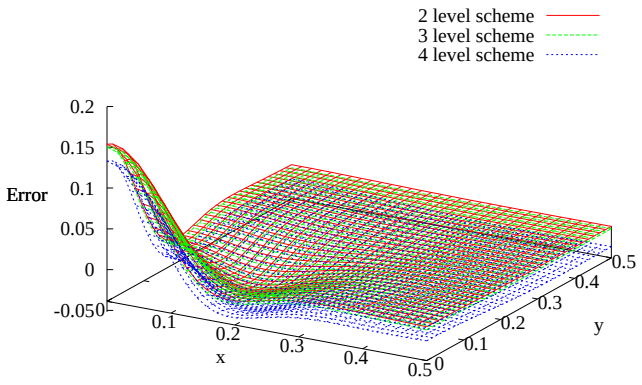


Figure 4: Error plot of the first quadrant for resolution $65^2$ and different number of coarsening levels.

This influence turns out to be not strong, i. e. the interface approximation of the FAC method is quite accurate. Additionally, the influence of the boundaries that are far enough away from the center may be negligible. The largest variation in the error norms for a different number of levels is around 15%.
In figure 4 a plot of the error for different numbers of grid levels is given. The error is largest at the origin, were also the solution has its peak and decays towards the interfaces. For the two and three level schemes the error is almost identical, while it is slightly shifted for the four-level scheme.
In total, coarsening with FAC-based schemes is efficient and accurate for the tested setup. The error behavior is as expected for a smooth right-hand side.

# 4 Conclusion and next steps

We showed a way to apply the FAC to open-boundary problems exemplary for Poisson's equation and developed an algorithm that utilizes the FAC for hierarchical coarsening. It was proved experimentally that the convergence properties of the FAC for the introduced class of problems are as good as those of a fully refined scheme which would require a way higher computational cost. We also analyzed the discretization errors for a typical MD setup and found the error order $\mathcal{O}(h^2)$.
The modified FAC provides a way to accurately solve problems on open domains with regular stencil operations. This makes it especially interesting for a parallel implementation on GPGPUs, where an irregular boundary treatment could be inefficient. A future implementation for this architecture should be able to treat 3D problems and be integrated in a more efficient framework that is based on compiled code.
The accuracy of the introduced approach shall be examined for more general cases: The error introduced by a non-smooth right-hand side should be analyzed in detail as well as the one caused by a jump in the dielectric constant $\varepsilon_0$. Since we plan to combine open boundary conditions in one dimension with periodic ones in the other we will observe how they interact. Finally, we plan to develop higher order schemes based on the FAC, replacing the five-point stencil.

# References


[1] M. Bolten. Hierarchical grid coarsening for the solution of the poisson equation in free space. *Electronic Transactions on Numerical Analysis*, 29:70–80, 2008.

[2] A. Brandt. Multi-level adaptive solutions to boundary-value problems. *Mathematics of Computation*, 31:333–390, 1977.

[3] H. Köstler. An accurate multigrid solver for computing singular solutions of elliptic problems. In *Abstracts Of the 12th Copper Mountain Conference on Multigrid Methods*, pages 1–11. SIAM, SIAM, Apr 2005.

[4] S. F. McCormick. *Multilevel Adaptive Methods for Partial Differential Equations*. Society for Industrial and Applied Mathematics, Philadelphia, PA, USA, 1989.

[5] U. Rüde. Fully Adaptive Multigrid Methods. 30(1):230–248, February 1993.

[6] U. Rüde. *Mathematical and computational techniques for multilevel adaptive methods*, volume 13 of *Frontiers in Applied Mathematics*. 1993.

[7] T Washio and C. W. Oosterlee. Error analysis for a potential problem on locally refined grids. *Numerische Mathematik*, 86(3):539–563, 2000.

[8] C. Zenger and H. Gietl. Improved difference schemes for the dirichlet problem of poisson's equation in the neighbourhood of corners. *Numerische Mathematik*, 30:315–332, 1978.